Enantioselectivity Reversal by Achiral Additives in the Soai Reaction: A Kinetic Understanding

Dominique Lavabre and Jean-Claude Micheau*

Laboratoire des IMRCP, UMR au CNRS No. 5623, Université Paul Sabatier, 118, Route de Narbonne, 31062 Toulouse Cedex, France

Jesús Rivera Islas and Thomas Buhse*

Centro de Investigaciones Químicas, Universidad Autónoma del Estado de Morelos, Av. Universidad 1001, Col. Chamilpa, 62209 Cuernavaca, Morelos, Mexico

Received: July 20, 2006; In Final Form: November 7, 2006

Numerical kinetic simulations have been employed to understand the origin of enantioselectivity reversal of chiral β-amino alcohol catalysts occurring in the presence of their achiral analogs in the autocatalytic addition of diisopropylzinc to pyrimidine carbaldehydes (Soai reaction). In a preceding work (Rivera Islas, J.; Lavabre, D.; Grevy, J. M.; Hernández Lamoneda, R.; Rojas Cabrera, H.; Micheau, J. C.; Buhse, T. *Proc. Natl. Acad. Sci. U.S.A.* **2005**, *102*, 13743−13748), we provided a possible explanation for the phenomenon of spontaneous mirror-symmetry breaking observed in this reaction. The effect of enantioselectivity reversal, giving rise to steep and abrupt transitions between opposed optically active states, has been identified by our current approach as another manifestation of such mirror-symmetry breaking capability. In the present case, we considered the involvement of the chiral catalyst and its achiral analog in the reaction network. Our modeling indicates that the enantioselectivity reversal can be either caused (i) by an interaction between the chiral and achiral additives or (ii) by an interaction of the customary products of the Soai reaction with the additives. The second option, which stands for the reversible inhibition of the chirally selective autocatalysts by the additives, could also explain a number of further additive effects in the Soai reaction reflecting the extraordinary sensitivity of this system toward the initial addition of almost any, even catalytically inactive, chiral substance.

I. Introduction

It has been assumed for decades that the origin of biomolecular homochirality[1] could be associated with basic principles of nonlinear kinetics in which small enantiomeric imbalances can be spontaneously amplified by means of autocatalytic reaction networks.[2] However, only very few experimental systems[3] have been identified so far to display chiral amplification by such nonlinear processing, and in most of these cases, their mechanism is still under investigation.[4]

Among those systems there is the so-called Soai reaction,[3b] i.e., the addition of diisopropylzinc to pyrimidine carbaldehydes that represents a unique example of spontaneous chiral amplification and mirror-symmetry breaking in organic chemistry.[5] Both effects arise essentially from autocatalytic kinetics in which the reaction product serves as an enantioselective catalyst for its proper formation. But besides the reaction product itself, a wide variety of organic and inorganic chiral additives were also observed to act as effective asymmetric inductors or catalysts in this reaction with an astonishingly high sensitivity.[6] The nature of impact of these additives, ranging as far as from α-amino acids to sodium chlorate crystals, remains elusive.

Recently, Soai and co-workers[7] reported a series of experiments using a chiral β-amino alcohol (*N,N*-dimethylnorephedrine) as the enantioselective catalyst and an achiral β-amino alcohol (*N,N*-dibutylaminoethanol) of similar chemical structure both added to the usual starting mixture of the Soai reaction. It was found that at a certain concentration of the achiral additive a reversal of the enantioselectivity of the chiral catalyst occurs: for example, the use of a pro-*R* catalyst[8] that usually yields a product with *R* configuration forms a product with *S* configuration if the achiral additive exceeds a specific concentration, and the opposite case was true for the use of a pro-*S* catalyst. The corresponding enantiomeric excess (ee) as a variation of the mole fraction of the added compounds revealed steep transitions between the two corresponding product configurations from almost ee $= +1$ to ee $= -1$ or vice versa (taking either the *R* or *S* configuration of the Soai reaction products as a reference). Thus, at a certain critical mole fraction of the additives the transitions between the two optically active states occurred practically without intermediate values of the ee.

The observed reversal of enantioselectivity indicates an involvement of the chiral and achiral additive in the overall reaction mechanism. Moreover, the steep transitions between the opposite configurations and the lack of intermediate values of the ee match the characteristics of a bifurcation scenario such as that observed in mirror-symmetry breaking transitions. Hence, a closer understanding of these phenomena could pave the way for a first perception of the diverse additive effects and its extraordinary sensitivities in the Soai reaction.

Previously, we have presented a kinetic modeling approach to account for the main properties of the Soai reaction.[4b] In the present paper, we will use the same core model with parameters

* Corresponding authors. Phone: +33561556275 (J.-C.M.). Fax: +33561558155-(J.-C.M.). Phone/fax: +527773297997 (T.B.). E-mail: micheau@chimie.ups-tlse.fr (J.-C.M.); buhse@uaem.mx (T.B.).

10.1021/jp064618s CCC: $37.00
Published on Web 12/14/2006

giving rise to mirror-symmetry breaking. Our purpose is to provide an explanation for the observed reversal of enantioselectivity from a kinetic point of view. We will examine the mechanistic assumptions of an interaction between the additives as well as an interaction between the additives and the customary Soai reaction products.

II. Kinetic Models

For our current study, we used a kinetic core model of the Soai reaction that gives rise to mirror-symmetry breaking transitions as the essential criterion but did not pay particular attention to mechanistic details that were assumed to have no significant effect on the global behavior of enantioselectivity reversal. As confirmed by our earlier approach,[4b] the main properties of the typical Soai reaction can be described by a comparatively simple kinetic core model that includes the assumption of spontaneous product formation (step 1), autocatalysis (steps 2 and 3) and dimerization of the isopropylzinc alkoxide product (steps 4−6) as the essential ingredients.

Core Model:

$$A + Z \rightarrow 0.5R + 0.5S \quad (k_0) \tag{1}$$

$$A + Z + R \rightarrow 2R \quad (k_1) \tag{2}$$

$$A + Z + S \rightarrow 2S \quad (k_1) \tag{3}$$

$$R + S \leftrightarrow RS \quad (k_2, k_3) \tag{4}$$

$$R + R \leftrightarrow RR \quad (k_4, k_5) \tag{5}$$

$$S + S \leftrightarrow SS \quad (k_4, k_5) \tag{6}$$

Here, A = pyrimidine carbaldehyde, Z = diisopropylzinc, R or S = enantiomeric zinc alkoxide, RR or SS = homochiral zinc alkoxide dimers, and RS = heterochiral zinc alkoxide dimer.

Accordingly, we have used for the present task the above kinetic core model standing for the original Soai reaction, i.e., without the involvement of any additive. In order to use the simplest model, alkoxide monomers (R or S) were assumed as autocatalytic species.[9] The values for the rate constants k_0−k_5 are the same as in our earlier paper[4b] and have been used as predetermined and fixed parameter values for all the simulations reported in the study, i.e., $[A]_0 = 0.02$ M, $[Z]_0 = 0.04$ M; $k_0 = 5.2 \times 10^{-3}$ M^{-1} s^{-1}, $k_1 = 69$ M^{-2} s^{-1}, $k_2 = 4.5 \times 10^5$ M^{-1} s^{-1}, $k_3 = 0.052$ s^{-1}, $k_4 = 4.8 \times 10^3$ M^{-1} s^{-1}, $k_5 = 21$ s^{-1}.

To account for the participation of chiral and achiral additives, supplementary kinetic steps have been considered in addition to the core model where two different scenarios A (additive−additive interactions) and B (additive−product interactions) have been assessed separately.

Scenario A. Scenario A represents interactions between the chiral and achiral additives as it has been suggested by Soai and co-workers.[7] The additives are allowed to form a variety of dimer species (steps A-1 to A-3) as well as to display catalytic activity in the formation of the products R and S (steps A-4 to A-6). In accordance with the proposed formation of a dimeric catalytic species that supports the generation of the enantiomer opposite to the chiral configuration of the catalyst,[7] the mixed aggregate XY in step A-5 is assumed to promote the product of opposite configuration to that of X.

$$X + X \leftrightarrow XX \quad (k_{6A}, k_{7A}) \tag{A-1}$$

$$X + Y \leftrightarrow XY \quad (k_{8A}, k_{9A}) \tag{A-2}$$

$$Y + Y \leftrightarrow YY \quad (k_{10A}, k_{11A}) \tag{A-3}$$

$$A + Z + XX \rightarrow (1 - a)R + aS + XX \quad (k_{12A}) \tag{A-4}$$

$$A + Z + XY \rightarrow (1 - b)R + bS + XY \quad (k_{13A}) \tag{A-5}$$

$$A + Z + YY \rightarrow (1 - c)R + cS + YY \quad (k_{14A}) \tag{A-6}$$

Here, X = chiral additive and Y = achiral additive both considered to be zinc alkoxides formed instantly by a rapid reaction between the corresponding β-amino alcohols and diisopropylzinc. The stereoselectivity coefficients *a*, *b*, and *c*, whose values can be 0, 0.5, or 1 for each, depend on the configuration of the additive. The following set of differential equations has been derived from scenario A:

$$dA/dt = dZ/dt = -k_0AZ - k_1RAZ - k_1SAZ - k_{12A}AZ(XX) - k_{13A}AZ(XY) - k_{14A}AZ(YY)$$

$$dR/dt = 0.5k_0AZ + k_1RAZ - k_2SR + k_3(SR) - 2k_4R^2 + 2k_5(RR) + (1 - a)k_{12A}AZ(XX) + (1 - b)k_{13A}AZ(XY) + (1 - c)k_{14A}AZ(YY)$$

$$dS/dt = 0.5k_0AZ + k_1SAZ - k_2SR + k_3(SR) - 2k_4S^2 + 2k_5(SS) + ak_{12A}AZ(XX) + bk_{13A}AZ(XY) + ck_{14A}AZ(YY)$$

$$dRS/dt = k_2SR - k_3(SR)$$

$$dRR/dt = k_4R^2 - k_5(RR)$$

$$dSS/dt = k_4S^2 - k_5(SS)$$

$$dX/dt = -2k_{6A}XX + 2k_{7A}(XX) - k_{8A}XY + k_{9A}(XY)$$

$$dY/dt = -2k_{10A}YY + k_{11A}(YY) - k_{8A}XY + k_{9A}(XY)$$

$$dXX/dt = k_{6A}XX - k_{7A}(XX)$$

$$dXY/dt = k_{8A}XY - k_{9A}(XY)$$

$$dYY/dt = k_{10A}YY - k_{11A}(YY)$$

Scenario B. Scenario B denotes the reversible interaction between the additives X and Y and the products R and S of the Soai reaction in which the resulting complexes XR, XS, YR, and YS (generated in steps B-1 to B-4) are regarded as catalytically inactive species; i.e., its formation results in an inhibition of the autocatalytic species R and S. Moreover, it is likely that the impact of the chiral aminoalcohol additives is not limited only to these dimerization equilibria since monomeric aminoalcohol Zn complexes are known as chiral catalysts for the alkylation of aldehydes by dialkylzinc.[10] For this reason, the catalytic steps B-5 and B-6 involving the catalytic additives

X and Y and the formation of the products R and S have been added:

$$X + R \leftrightarrow XR \qquad (k_{6B}, k_{7B}) \qquad \text{(B-1)}$$

$$X + S \leftrightarrow XS \qquad (k_{8B}, k_{9B}) \qquad \text{(B-2)}$$

$$Y + R \leftrightarrow YR \qquad (k_{10B}, k_{11B}) \qquad \text{(B-3)}$$

$$Y + S \leftrightarrow YS \qquad (k_{12B}, k_{13B}) \qquad \text{(B-4)}$$

$$A + Z + X \rightarrow (1 - d)R + dS + X \qquad (k_{14B}) \qquad \text{(B-5)}$$

$$A + Z + Y \rightarrow (1 - e)R + eS + Y \qquad (k_{15B}) \qquad \text{(B-6)}$$

Here, d and e are stereoselectivity coefficients depending on the chiral or achiral character of X and Y. The following set of differential equations has been derived from scenario B:

$$dA/dt = dZ/dt = -k_0AZ - k_1RAZ - k_1SAZ - k_{14B}XAZ - k_{15B}YAZ$$

$$dR/dt = 0.5k_0AZ + k_1RAZ - k_2SR + k_3(SR) - 2k_4R^2 + 2k_5(RR) + (1 - d)k_{14B}XAZ + (1 - e)k_{15B}YAZ - k_{6B}XR + k_{7B}(XR) - k_{10B}YR + k_{11B}(YR)$$

$$dS/dt = 0.5k_0AZ + k_1SAZ - k_2SR + k_3(SR) - 2k_4S^2 + 2k_5(SS) + dk_{14B}XAZ + ek_{15B}YAZ - k_{8B}XS + k_{9B}(XS) - k_{12B}YS + k_{13B}(YS)$$

$$dRS/dt = k_2SR - k_3(SR)$$

$$dRR/dt = k_4R^2 - k_5(RR)$$

$$dSS/dt = k_4S^2 - k_5(SS)$$

$$dX/dt = k_{7B}(XR) + k_{9B}(XS) - k_{6B}XR - k_{8B}XS$$

$$dY/dt = k_{11B}(YR) + k_{13B}(YS) - k_{10B}YR - k_{12B}YS$$

$$dXR/dt = k_{6B}XR - k_{7B}(XR)$$

$$dXS/dt = k_{8B}XS - k_{9B}(XS)$$

$$dYR/dt = k_{10B}YR - k_{11B}(YR)$$

$$dYS/dt = k_{12B}YS - k_{13B}(YS)$$

Both scenarios A and B were evaluated by numerical simulations using arbitrarily chosen but chemically realistic rate parameter values. As already described elsewhere,[4b] kinetic modeling was carried out numerically by rigorously considering the full range of interrelated processes. The numerical integration was based on a semi-implicit fourth-order Runge−Kutta method with stepwise control for stiff ordinary differential equations that was sufficiently robust and reliable for nonlinear problems of the present case.

III. Results and Discussion

1. Enantioselectivity Reversal. As a central result of our approach, Figure 1 shows the effect of enantioselectivity reversal reproduced by the kinetic core model that has been improved by the proposed involvement of the chiral and achiral additives. Particularly, either the consideration of scenario A or scenario B in addition to the core model can lead to the type of step diagram showing steep transitions between the optically active states. However, as outlined in the following, the kinetic conditions are specifically distinct in both cases.

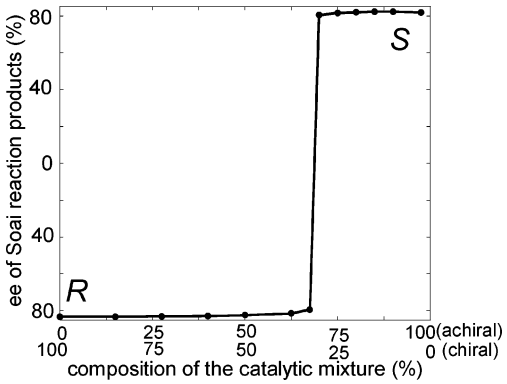

Figure 1. Simulation of enantioselectivity reversal in the Soai reaction (according to ref 7). Scenarios A and B in combination with the core model ($k_0 = 5.2 \times 10^{-3}$ M^{-1} s^{-1}, $k_1 = 69$ M^{-2} s^{-1}, $k_2 = 4.5 \times 10^5$ M^{-1} s^{-1}, $k_3 = 0.052$ s^{-1}, $k_4 = 4.8 \times 10^3$ M^{-1} s^{-1}, $k_5 = 21$ s^{-1}) give rise to the same result; hence, only one curve has been displayed. Scenario A ($[X]_0 + [Y]_0 = 4 \times 10^{-3}$ M): $k_{6A} = k_{8A} = k_{10A} = 1 \times 10^4$ M^{-1} s^{-1}, $k_{7A} = k_{9A} = k_{11A} = 100$ s^{-1}, $k_{12A} = 1.8$ M^{-2} s^{-1}, $k_{13A} = k_{14A} = 1$ M^{-2} s^{-1}, $a = 0$; $b = 1$; $c = 0.5$. Scenario B, simplest case: $[X]_0$ is varied from 0 to 4×10^{-3} M with $k_{6B} = 3.1$ M^{-1} s^{-1}, $k_{7B} = 0.032$ s^{-1}, $k_{8B} = 2.8$ M^{-1} s^{-1}, $k_{9B} = 0.025$ s^{-1}, $k_{10B} = k_{11B} = k_{12B} = k_{13B} = k_{14B} = k_{15B} = 0$. Scenario B, general case: $[X]_0 + [Y]_0 = 4 \times 10^{-3}$ M; $k_{6B} = 4.423 \times 10^4$ M^{-1} s^{-1}; $k_{8B} = 1 \times 10^4$ M^{-1} s^{-1}; $k_{10B} = k_{12B} = 2.05 \times 10^4$ M^{-1} s^{-1}; $k_{14B} = 0.06$ M^{-2} s^{-1}; $k_{15B} = 0.035$ M^{-2} s^{-1}; $k_{7B} = k_{9B} = k_{11B} = k_{13B} = 100$ s^{-1}; $d = 0$ and $e = 0.5$.

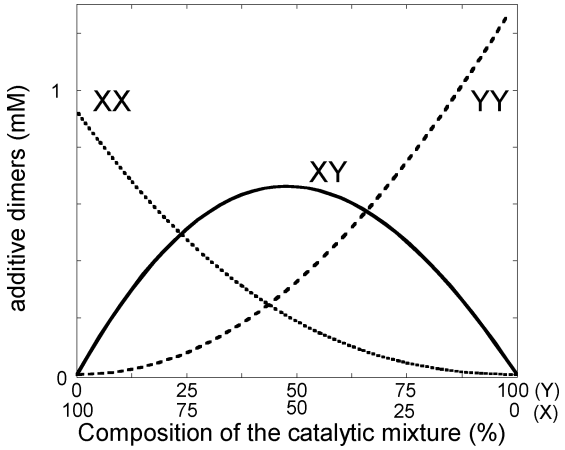

Figure 2. Illustration of an arbitrary equilibrium distribution of XX, XY, and YY dimers vs the composition of the catalytic mixture in scenario A from processes A-4 to A-6. ($k_{6A} = 2 \times 10^4$ M^{-1} s^{-1}, $k_{8A} = 10^5$ M^{-1} s^{-1}, $k_{10A} = 7 \times 10^4$ M^{-1} s^{-1}, and $k_{7A} = k_{9A} = k_{11A} = 10^2$ s^{-1}).

Assuming in scenario A reversible interactions between the chiral and achiral additives, the resulting equilibrium distribution of the dimers XX, XY, and YY depends only on their relative stabilities since the products R or S are not involved in their formation.

Figure 2 shows a prototype equilibrium distribution that essentially is able to promote the effect of enantioselectivity reversal. In this case, at a high concentration of X, step A-1 is active and provides a large amount of XX dimers while the catalytic process A-4 generates the product with the same configuration of X. In contrast, at a high concentration of Y, the association A-2 becomes more active and provides a large amount of mixed XY aggregates which initiate the catalytic step

A-5 that is assumed to provide the product with opposite configuration to X.

Depending on the relative catalytic strength and stereoselectivity of each of the dimers XX, XY, and YY, step diagrams of the type shown in Figure 1 can be readily obtained. However, as already pointed out by Soai and co-workers,[7] the hybrid catalyst XY has to be considered to promote the product of opposite configuration. Moreover, it is implicated that dimers, i.e., XX, XY, and YY, and not monomers such as X or Y are the catalytically active species which is not in accordance with the commonly accepted mechanism for typical dialkylzinc additions to aldehydes catalyzed by β-amino alcohols.[10] For this reason, we extended our approach to evaluate an alternate scenario B.

Assuming in scenario B reversible interactions between the Soai reaction products R and S and the "pro-*R*" chiral additive X (steps B-1 and B-2), we found that these association equilibria consisting of only 2 steps were sufficient to induce the reversal of enantioselectivity. It was not essential to consider the presence of the achiral additive Y to reproduce the enantioselectivity reversal. Hence, in this simplest case, the scenario B does not even require the achiral additive that would only play the role to dilute the chiral additive. Considering the addition of X to the reaction mixture, the R and S enantiomers then become partially trapped to form XR and XS complexes. As a result of possible diastereomeric effects, XR and XS may display different rates of formation and dissociation as well as different thermodynamic stabilities that may cause a shift in the ratio between the alkoxide enantiomers provided by the typical Soai reaction. This effect occurs already when the diastereomeric recognition ability of X versus R or S is very small, i.e., even if the respective association rate constants k_{6B} and k_{8B} differ less than 10^{-11} M^{-1} s^{-1}.

The trapping of the Soai reaction products results in a poisoning of the autocatalysts R and S that are partially withdrawn from the autocatalytic cycle of the core mechanism. Consequently, the enantiomer that is trapped stronger is also the one that is poisoned stronger so that the weaker trapped enantiomer governs the process and can imprint its chiral configuration on the final outcome of the reaction. This could be the origin of the enantioselectivity reversal.

To enlighten the effect of the association equilibria B-1 and B-2, we simulated the time evolution of XS and XR starting from an equimolar mixture of R and S and in the presence of X but without the influence of the core reaction, i.e., without the involvement of processes 1−6, for the hypothetical case in which the Soai reaction is not operating. As shown in Figure 3, the most interesting situation occurs when the thermodynamically most stable complex, here chosen arbitrarily to be XS, is on the other hand the slower one to be formed. Under such a condition, the two kinetic curves for the time evolution of XS and XR give rise to an intersection where at the beginning of the process more R than S is present in complexed form (XR > XS) while during the later stages S exceeds the presence of R (XR < XS). Numerical simulations show that the position of the intersection depends on the concentration of X and occurs earlier when the concentration of X increases. For the case that the most stable complex is also the faster one to be formed no intersection of the kinetic curves takes place; i.e., the enantiomeric direction remains the same for all concentrations of the additive. Such a situation could be at the origin of the miscellaneous additive effects displayed by a great number of chiral substances in the Soai reaction.

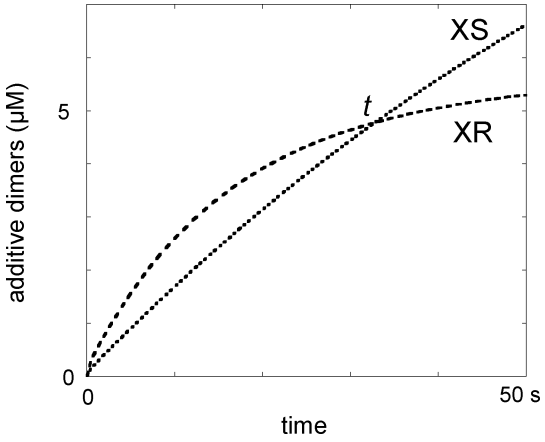

Figure 3. Typical time evolution of the XS and XR complexes obtained by the simulation of the association equilibria B-1 and B-2 alone. The intersection (t) of the two curves denotes the time at which the predominance of the respective complex species overturns. This turning point occurs earlier when the concentration of X increases. In this simulation, the thermodynamically less stable complex is kinetically favored by taking $k_{6B} > k_{8B}$ and $k_{7B} > k_{9B}$ but $k_{6B}/k_{7B} < k_{8B}/k_{9B}$ (k_{6B} = 20 M^{-1} s^{-1}, $k_{7B} = 6 \times 10^{-2}$ s^{-1}, k_{8B} = 10 M^{-1} s^{-1}, $k_{9B} = 10^{-2}$ s^{-1}).

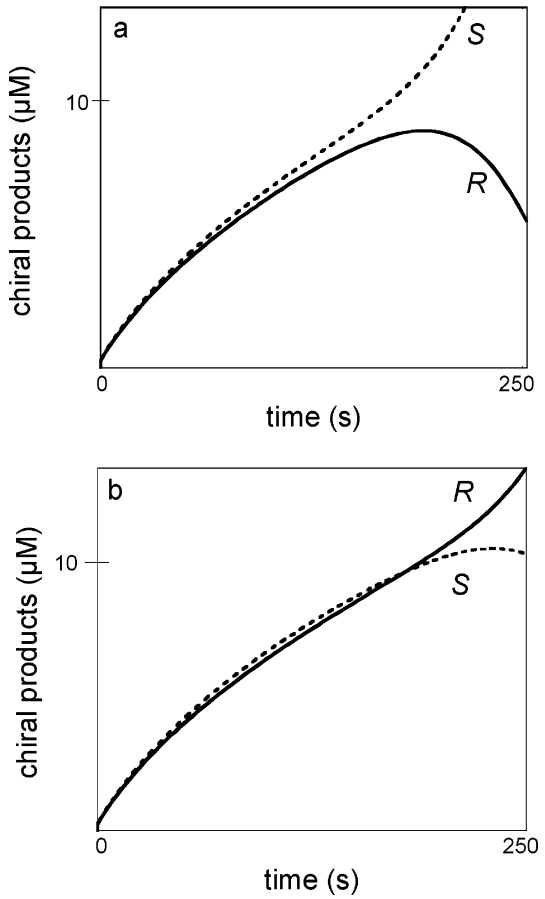

Figure 4. Typical time evolution of the Soai reaction products R and S under consideration of the association equilibria B-1 and B-2 and the kinetic core model ($k_0 = 5.2 \times 10^{-3}$ M^{-1} s^{-1}, k_1 = 69 M^{-2} s^{-1}, $k_2 = 4.5 \times 10^5$ M^{-1} s^{-1}, k_3 = 0.052 s^{-1}, $k_4 = 4.8 \times 10^3$ M^{-1} s^{-1}, k_5 = 21 s^{-1}, k_{6B} = 10.6 M^{-1} s^{-1}, k_{7B} = 0.013 s^{-1}, k_{8B} = 10 M^{-1} s^{-1} and k_{9B} = 0.01 s^{-1}). (a) $[X]_0 = 1.6 \times 10^{-3}$ M: evolution toward S. (b) $[X]_0 = 1.7 \times 10^{-3}$ M: evolution toward R.

We will now consider the coupling of the equilibria B-1 and B-2 with the core reaction (steps 1−6), again assuming that XS is thermodynamically but not kinetically favored (Figure

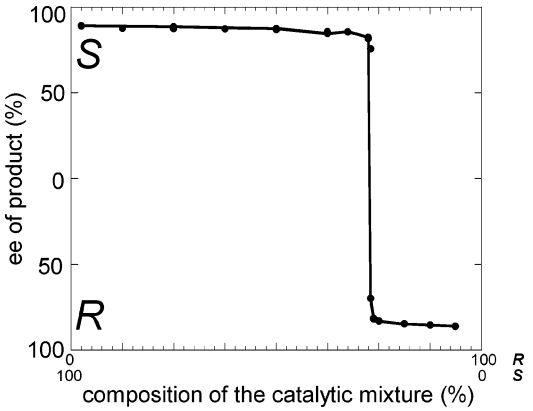

Figure 5. Enantioselectivity reversal in the presence of two competing almost enantiomeric catalysts (according to ref 11). In this case, for the full model scenario B (steps B-1 to B-6) both X and Y were considered as chiral catalysts where X = pro-*R* and Y = pro-*S*. The parameters for the interactions between the additives and the Soai reaction products k_{6B}, k_{8B}, k_{10B}, and k_{12B} have been chosen to respect the expected ranking for such chirally selective processes. Parameters: all cases, $k_0 = 5.2 \times 10^{-3}$ M^{-1} s^{-1}, $k_1 = 69$ M^{-2} s^{-1}, $k_2 = 4.5 \times 10^5$ M^{-1} s^{-1}, $k_3 = 0.052$ s^{-1}, $k_4 = 4.8 \times 10^3$ M^{-1} s^{-1}, $k_5 = 21$ s^{-1}. Scenario A: $k_{6A} = 2 \times 10^4$ M^{-1} s^{-1}, $k_{8A} = 1 \times 10^5$ M^{-1} s^{-1}, $k_{10A} = 7 \times 10^4$ M^{-1} s^{-1}, $k_{7A} = k_{9A} = k_{11A} = 100$ s^{-1}, $k_{12A} = 0.03$ M^{-2} s^{-1}, $k_{13A} = 0.05$ M^{-2} s^{-1}, $k_{14A} = 0.15$ M^{-2} s^{-1}, $a = 0$, $b = 0.5$, $c = 1$. Scenario B: $k_{6B} = 1.4 \times 10^4$ M^{-1} s^{-1}, $k_{8B} = 9 \times 10^3$ M^{-1} s^{-1}, $k_{10B} = 1 \times 10^4$ M^{-1} s^{-1}, $k_{12B} = 1.1 \times 10^4$ M^{-1} s^{-1}, $k_{14B} = 0.04$ M^{-2} s^{-1}, $k_{15B} = 0.08$ M^{-2} s^{-1}, $k_{7B} = k_{9B} = k_{11B} = k_{13B} = 100$ s^{-1}, $d = 0$; $e = 1$. Both scenarios A and B give the same result; hence, only one curve has been displayed.

4). Due to the autocatalytic feedback, the Soai reaction is sensitive to virtually any tiny initial ee in R or S. Hence it is expected that in the early stage of reaction the product configuration will be directed toward S because more R than S is trapped in complexed form (XR > XS). However, by reaching a critical time at which the intersection (*t* in Figure 3) between the kinetic curves occurs, the contrary happens, and now the formation of R is favored (XR < XS). Depending on the dynamics of the Soai reaction and its amplification effect, the influence of this reversal after the critical time can be imprinted into the actual outcome of the reaction or not. When the concentration of X is small, this critical time is delayed and the final product configuration of the Soai reaction has been already imprinted toward S; i.e., enantioselectivity reversal occurs. On the other hand, when the concentration of X is high, the critical time is shorter and the final product configuration is imprinted toward R. Figure 4 illustrates the evolution of R and S when the association equilibria B-1 and B-2 are coupled with the typical Soai reaction. The graphs a and b correspond to close points on both sides of the ee transition.

2. Shift of Transition Step under Structural Variation of the Achiral Additive. It has been observed by Soai and co-workers that the transitions between the optically active states were shifting and occurred at different mole fractions under slight variations of the chemical structure of the achiral additive,[7] i.e., from dibutyl to dimethylaminoethanol. The consideration of the core model coupled to steps B-1 to B-6 and the relation X + Y = constant, provided us the sufficient elements to reproduce this effect. In our simulations, the shift in the transition under keeping its characteristic steep slope was either obtained by varying the catalytic efficiency of the achiral additive Y (k_{15B}) by a factor less than 10 or by varying the interaction between Y and the products R and S ($k_{10B} = k_{12B}$ and $k_{11B} = k_{13B}$) by a factor of less than 2. For symmetry reasons, the association of the achiral additive Y to R and S occurs equally valued.

Also with scenario A it was possible to reproduce the above effect by varying the parameters related to the achiral additive interactions (k_{10A} or k_{8A}) or the catalytic efficiency of the mixed dimer XY (k_{13A}) by factors less than 50.

3. Enantioselectivity Reversal in the Presence of Competing Catalysts. In an independent and preceding study, Soai and co-workers analyzed their system by simultaneously adding pro-*R* and pro-*S* β-amino alcohol catalysts (*N*,*N*-dialkylnorephedrines) to the reaction mixture where both additives slightly differed in their structure.[11] Variations in the mole fraction resulted again in transitions between the optically active states of the corresponding products. Basically, the predominance of the pro-*R* catalyst resulted in products with *R* configuration and the opposite happened for the pro-*S* catalyst. The transitions did not necessarily occur at equimolar proportions of both catalysts indicating different catalytic efficiencies. As shown in Figure 5, these experimental observations can also be reproduced by considering the full scenario B as well as by scenario A.

For scenario A, it was assumed that catalysis by the *meso*-complex XY was not stereoselective, hence $b = 0.5$. For the simulations of scenario B, it was now assumed that X (a pro-*R* with $d = 0$) and Y (a pro-*S* with $e = 1$) stand for the almost enantiomeric catalysts, both displaying similar catalytic activities in the product formation while their recognition capacities were considered to be slightly different in a way that X interacts stronger with R (i.e., $k_{6B} > k_{8B}$) and Y stronger with S (i.e., $k_{12B} > k_{10B}$). This is reasonable given that X and Y are not strictly enantiomers.

IV. Conclusion

In this paper, we have used a symmetry-breaking kinetic model of the Soai reaction with arbitrarily chosen rate parameters and examined two hypotheses to account for the effect of enantioselectivity reversal: (i) the additive−additive interaction with corresponding specific catalytic activity of the resulting dimer species (scenario A) and (ii) the additive−product interaction resulting in the inhibition of the autocatalytic products of the Soai reaction (scenario B). With both assumptions, we could reproduce additive induced steplike diagrams that have been observed experimentally. Several constraints related to the relative stabilities of the various complex species and their kinetics of formation and dissociation as well as the importance of the relative stereoselectivities of the catalytic steps have been emphasized.

It appears that almost any chiral substance is able to act as a chiral inductor in the Soai reaction. All these additive effects cannot be reproduced by model scenario A because it is not known that all of those chiral compounds bear catalytic properties. On the other hand, it is always possible that there exist weak interactions between the products R and S and the chiral additive as we have proposed in model scenario B. This scenario predicts that a very slight kinetic or thermodynamic difference in the interaction between the chiral additive and each of the both reaction products is sufficient to drive the reaction into a certain enantiomeric direction. Hence the occurrence of interactions between the reaction products and the additives as proposed by scenario B could not only shed light on the origin of steplike diagrams but also provide a tentative kinetic explanation for the variety of chiral additive effect in the Soai reaction.

References and Notes

(1) (a) De Min, M.; Levy, G.; Micheau, J. C. *J. Chim. Phys.* **1988**, *85*, 603−619. (b) Bonner, W. A. *Origins Life Evol. Biosphere* **1991**, *21*, 59−

111. (c) Keszthely, L. *Q. Rev. Biophys.* **1995**, *28*, 473−507. (d) Siegel, J. S. *Chirality* **1998**, *10*, 24−27. (e) Avalos, M.; Babiano, R.; Cintas, P.; Jiménez J. L.; Palacios, P. C. *Tetrahedron: Asymmetry* **2000**, *11*, 2845−2874. (f) Sandars, P. G. H. *Int. J. Astrobiol.* **2005**, *4*, 49−61.

(2) (a) Frank, F. C. *Biochim. Biophys. Acta* **1953**, *11*, 459−463. (b) Calvin, M. *Molecular Evolution*; Oxford University Press: Oxford, 1969. (c) Seelig, F. F. *J. Theor. Biol.* **1971**, *31*, 355−361. (d) Decker, P. In *Origins of Optical Activity in Nature*; Walker, D. C., Ed.; Elsevier: Amsterdam, 1979; pp 109−124. (e) Kondepudi, D. K.; Nelson, G. W. *Physica A* **1984**, *125*, 465−496.

(3) (a) Kondepudi, D. K.; Kaufman, R. J.; Singh, N. *Science* **1990**, *250*, 975−976. (b) Soai, K.; Shibata, T.; Morioka, H; Choji, K. *Nature* **1995**, *378*, 767−768. (c) Asakura, K.; Kobayashi, K.; Mizusawa, Y.; Ozawa, T.; Osanai, S.; Yoshikawa, S. *Physica D* **1995**, *84*, 72−78. (d) Kondepudi, D. K.; Laudatio, J.; Asakura, K. *J. Am. Chem. Soc.* **1999**, *121*, 1448−1451.

(4) (a) Blackmond, D. G. *Proc. Natl. Acad. Sci. U.S.A.* **2004**, *101*, 5732−5736. (b) Rivera Islas, J.; Lavabre, D.; Grevy, J. M.; Hernández Lamoneda, R.; Rojas Cabrera, H.; Micheau, J. C.; Buhse, T. *Proc. Natl. Acad. Sci. U.S.A.* **2005**, *102*, 13743−13748. (c) Viedma, C. *Phys. Rev. Lett.* **2005**, *94*, 065504. (d) Plasson, R.; Kondepudi, D. K.; Asakura, K. *J. Phys. Chem. B* **2006**, *110*, 8481−8487.

(5) (a) Soai, K.; Shibata, T.; Sato, I. *Acc. Chem. Res.* **2000**, *33*, 382−390. (b) Sato, I.; Urabe, H.; Ishiguro, S.; Shibata, T.; Soai, K. *Angew. Chem., Int. Ed.* **2003**, *42*, 315−317. (c) Soai, K.; Sato, I.; Shibata, T.; Komiya, S.; Hayashi, M.; Matsueda, Y.; Imamura, H.; Hayase, T.; Morioka, H.; Tabira, H.; Yamamoto, J.; Kowata, Y. *Tetrahedron: Asymmetry* **2003**, *14*, 185−188. (d) Singleton, D. A.; Vo, L. K. *Org. Lett.* **2003**, *5*, 4337−4339. (e) Gridnev, I. D.; Serafimov, J. M.; Quiney, H.; Brown, J. M. *Org. Biomol. Chem.* **2003**, *1*, 3811−3819. (f) Soai, K.; Kawasaki, T. *Chirality* **2006**, *18*, 469−478.

(6) (a) Shibata, T.; Yamamoto, J.; Matsumoto, N.; Yonekubo, S.; Osanai, S.; Soai, K. *J. Am. Chem. Soc.* **1998**, *120*, 12157−12158. (b) Soai, K.; Osanai, S.; Kadowaki, K.; Yonekubo, S.; Shibata, T.; Sato, I. *J. Am. Chem. Soc.* **1999**, *121*, 11235−11236. (c) Sato, I.; Kadowaki, K.; Soai, K. *Angew. Chem., Int. Ed.* **2000**, *39*, 1510−1512. (d) Sato, I.; Yamashima, R.; Kadowaki, K.; Yamamoto, J.; Shibata, T.; Soai, K. *Angew. Chem., Int. Ed.* **2001**, *40*, 1096−1098. (e) Soai, K.; Sato, I. *Chirality* **2002**, *14*, 548−554. (f) Sato, I.; Sugie, R.; Matsueda, Y.; Furumura, Y.; Soai, K. *Angew. Chem., Int. Ed.* **2004**, *43*, 4490−4492. (g) Kawasaki, T.; Jo, K.; Igarashi, H.; Sato, I.; Nagano, M.; Koshima, H.; Soai, K. *Angew. Chem., Int. Ed.* **2005**, *44*, 2774−2777. (h) Kawasaki, T.; Suzuki, K.; Hatase, K.; Otsuka, M.; Koshima, H.; Soai, K. *Chem. Commun.* **2006**, 1869−1871.

(7) Lutz, F.; Igarashi, T.; Kawasaki, T.; Soai, K. *J. Am. Chem. Soc.* **2005**, *127*, 12206−12207.

(8) In the following, we call "pro-*R*" an additive (catalytic or not) that directs the Soai reaction towards an *R* configuration when sufficiently concentrated.

(9) We have verified that the consideration of zinc alkoxide dimers as catalytic species expressed by the kinetic steps (I) A + Z + RR → R + RR, (II) A + Z + SS → S + SS, and (III) A + Z + RS → 0.5S + 0.5R + RS instead of steps 2 and 3 of the core model can lead to very similar simulation results as presented in our current study.

(10) (a) Kitamura, M.; Yamakawa, M.; Oka, H.; Suga, S.; Noyori, R. *Chem. Eur. J.* **1996**, *2*, 1173−1181. (b) Noyori, R.; Suga, S.; Oka, H.; Kitamura, M. *Chem. Rec.* **2001**, *1*, 85−100.

(11) Lutz, F.; Sato, I.; Soai, K. *Org. Lett.* **2004**, *6*, 1613−1616.